

## Porphyrin-templated synthetic G-quartet (PorphySQ): a second prototype of G-quartet-based G-quadruplex ligand†

Hai-Jun Xu, Loic Stefan, Romain Haudecoeur, Sophie Vuong, Philippe Richard, Franck Denat, Jean-Michel Barbe, Claude P. Gros\* and David Monchaud\*

Received 22nd March 2012, Accepted 17th May 2012

DOI: 10.1039/c2ob25601k

Template-assembled synthetic G-quartet (TASQ) has been reported recently as a G-quadruplex ligand interacting with DNA according to an unprecedented, nature-inspired ‘like likes like’ approach, based on the association between two G-quartets, one being native (quadruplex) and the other one artificial (ligand). Herein, a novel TASQ-based ligand is designed, synthesized and its quadruplex-recognition properties are evaluated *in vitro*: PorphySQ (for porphyrin-templated synthetic G-quartet) displays enhanced quadruplex recognition properties as compared to the very first reported prototype (DOTASQ, for DOTA-templated synthetic G-quartet), since the porphyrin template insures a more stable intramolecular G-quartet fold due to self-stabilizing interactions that may take place intramolecularly between the porphyrin ring and the formed G-quartet.

## Introduction

Guanine is a very versatile nucleobase due to a highly malleable H-bond creating capability, *via* both its Watson–Crick and Hoogsteen edges (Fig. 1).<sup>1</sup> Only the former is involved in the formation of the guanine–cytosine base pair (Fig. 1) while both the former and latter participate in the creation of alternative assemblies, including base triplets (the basic building blocks of triplex-DNA),<sup>2</sup> quartets (notably G-quartets, a planar array of four guanines (Fig. 1), the basic building blocks of quadruplex-DNA, *vide infra*), and supramolecular higher-order structures like linear ribbons (Fig. 1) or helical foldamers (for a virtually unlimited number of guanines).<sup>3</sup>

The spontaneous self-assembly property of guanines makes them occupy a special place in the nucleic acids community since it enables the oligonucleotides to which the guanines belong to adopt peculiar secondary structures: among them, G-quadruplex-DNA has recently attracted outstanding attention.<sup>4</sup> G-rich oligonucleotides are indeed able to form G-quartets (intra- or inter-molecularly); in the case of contiguous guanine stretches, the resulting juxtaposed G-quartets, self-stabilized by both  $\pi$ -stacking interactions and physiologically relevant cation trapping, form the columnar frame of a four-stranded DNA

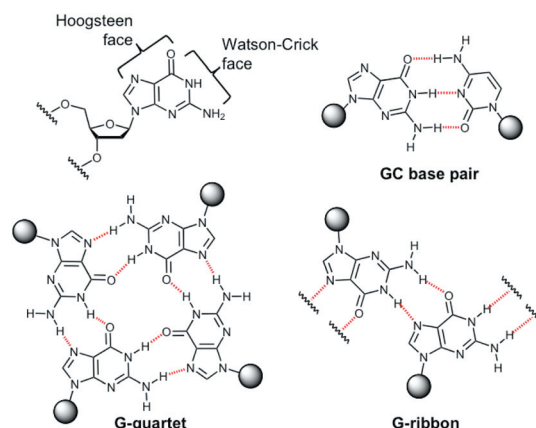


**Fig. 1** Schematic representation of the guanine base H-bond donor/acceptor capability; schematic representation of a GC base pair, a G-quartet and a G-ribbon.

structure termed as G-quadruplex-DNA.<sup>5</sup> Putative quadruplex-forming DNA sequences are widely dispersed in the genome,<sup>6</sup> but are particularly enriched in key regions such as telomeres<sup>7</sup> and promoters of oncogenes;<sup>8</sup> G-quadruplex-RNA is also increasingly studied, notably because the 5'-untranslated regions (5'-UTR) of mRNA are enriched in quadruplex-forming RNA sequences.<sup>9</sup> Consequently, it has been attempted to control the corresponding physiological events (*i.e.* the chromosomal stability (telomeric quadruplexes) and the regulation of gene expression at both the transcriptional (quadruplex-DNA in promoter) and translational (5'-UTR) levels) by small-molecules

Institut de Chimie Moléculaire, CNRS UMR6302, Université de Bourgogne, Dijon, France. E-mail: [claud.gros@u-bourgogne.fr](mailto:claud.gros@u-bourgogne.fr); [david.monchaud@u-bourgogne.fr](mailto:david.monchaud@u-bourgogne.fr); Fax: (+33) 380 396 117; Tel: (+33) 380 396 112 (CPG); (+33) 380 399 043 (DM)

† Electronic supplementary information (ESI) available: chemical synthesis and characterizations (including <sup>1</sup>H-NMR and HRMS-ESI spectra) of PorphySQ. See DOI: 10.1039/c2ob25601k

displaying high affinity and selectivity for quadruplex (G-quadruplex ligands). The intensive quest of G-quadruplex ligands has provided several promising candidates,<sup>10</sup> among which telomestatin,<sup>11</sup> BRACO-19,<sup>12</sup> RHPS4,<sup>13</sup> Phen-DC<sup>14</sup> and Pyridostatin<sup>15</sup> can be cited; most of them have been designed and studied as quadruplex-DNA interacting compounds,<sup>10,16</sup> but examples of quadruplex-RNA ligands are currently emerging.<sup>9,17</sup> Importantly, in the vast majority of cases, these ligands are fine-tuned from the known pool of duplex-ligands, according to established guidelines (*viz.* extended aromatic core with water-solubilising cationic nitrogen moieties).<sup>16</sup>

We recently reported on an original design of a G-quartet-based quadruplex ligand named DOTASQ (for DOTA-templated synthetic G-quartet, Fig. 2),<sup>18</sup> thereby expanding the family of TASQ (for template-assembled synthetic G-quartet)<sup>19</sup> using DOTA (for 1,4,7,10-tetraazacyclododecane-*N,N',N'',N'''*-tetraacetic acid) as an alternative template to the previously used calixarene<sup>20</sup> and macrocyclopeptide.<sup>21</sup> The logic behind using a synthetic G-quartet is to mimic the naturally occurring self-assembly of contiguous G-quartets that is at the origin of the quadruplex stability. This approach is based on the association between two G-quartets, one being natural (quadruplex) and the other synthetic (TASQ), according to a 'like likes like' process. It was however limitedly successful since DOTASQ itself was not a good ligand *per se* (*vide infra*), but its corresponding terbium complex displayed satisfying quadruplex-interacting properties (fair affinity, exquisite selectivity). This originates in the stability of the intramolecular G-quartet fold: NMR studies have indeed highlighted that the equilibrium between the *closed* (*i.e.* the G-quartet is formed) and *open* (*i.e.* the G-quartet is not formed) conformations of DOTASQ as a free base is shifted in solution toward the open form (in an ~2 : 8 ratio); the insertion of a metal inside the DOTA cavity of the DOTASQ forces the four guanines to be on the same side of the template, thereby favouring the G-quartet formation and so, improving the G-quadruplex recognition ability. We thus believe that one way to improve the proficiency of G-quartet-based G-quadruplex ligands is to design TASQ with a higher-stability G-quartet:

herein we report on a TASQ in which the template not only promotes but also – and above all – stabilizes the G-quartet once formed (this intramolecular  $\pi$ -stacking stabilization is symbolized by the red arrow in Fig. 2). To this end, we used a porphyrin template since *i*- it offers the *ad hoc*  $C_4$ -symmetry required for the introduction of four guanine arms, and *ii*- it is a widely studied and efficient G-quartet interacting scaffold (TMPyP4 is one of the most emblematic examples).<sup>22</sup> We thus herein report on the design of a porphyrin-templated synthetic G-quartet (PorphySQ, Fig. 2) *via* semi-empirical calculations, its synthesis and the evaluation of its quadruplex-recognition properties (*via* a comparative analysis of FRET-melting results of both DOTASQ and PorphySQ).

## Results and discussion

### Design and molecular modelling

The structure of PorphySQ was first studied *in silico*; a particular attention was paid to the length of the connecting arms between the template (in red, Fig. 2) and the guanine (in black, Fig. 2). With DOTASQ, a 12-atom link was found long enough to enable the G-quartet fold. The porphyrin ring being broader than the DOTA cycle (16- vs. 12-membered ring respectively), we envisioned that a shorter arm (9- vs. 12-atom link respectively) may be used for constructing the PorphySQ skeleton, in order to limit the hydrophobicity imparted by long  $\text{CH}_2$  stretches. The ability of the thus designed PorphySQ to adopt the closed conformation was *in silico* investigated. To this end, a semi-empirical method, using the RM1 Hamiltonian,<sup>23</sup> was employed to perform energy minimization studies: as shown in Fig. 3, a nearly flat G-quartet is formed, at 6.5 Å above the porphyrin plane. The general pattern obtained for the G-quartet is similar

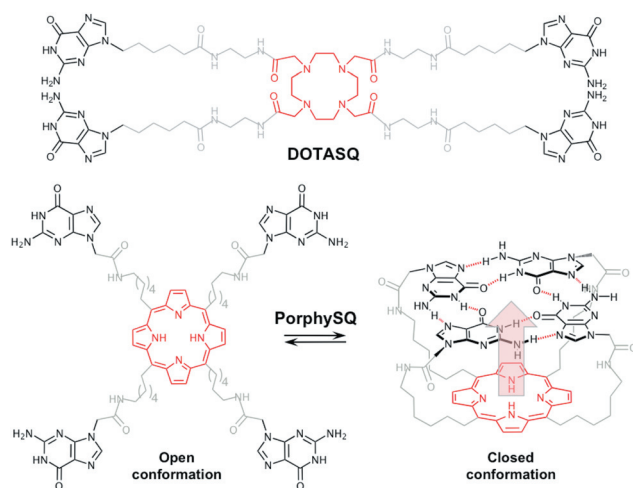


**Fig. 2** Chemical structures of DOTASQ (upper panel) and PorphySQ (lower panel) and schematic representation of its *open* (left) and *closed* (right) conformation.

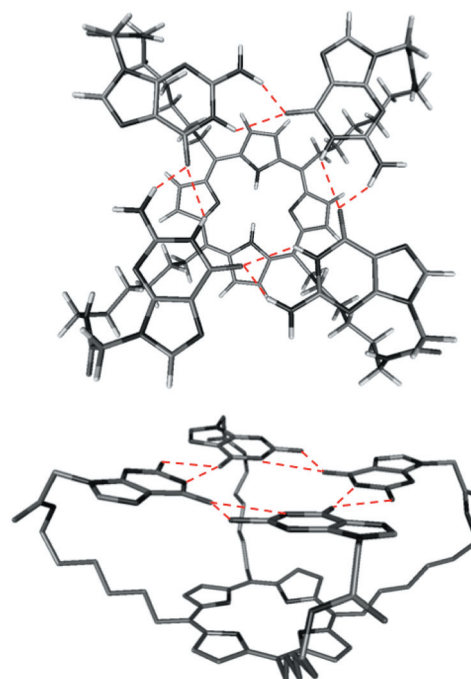


**Fig. 3** Top- (upper panel) and side-view (lower panel) of the energy-minimized (RM1) structure of PorphySQ.

to that of the previously minimized one *via* a B3LYP DFT study.<sup>24</sup> Given that calculations are performed *in vacuo* and in a cation-free environment, the H-bond network is different to what is usually determined for G-quadruplex-DNA (schematically represented in Fig. 1): indeed, with both RM1 (this study) and B3LYP calculations, the guanine interactions take place *via* H-bonds created between one carbonyl group and 2 N–H hydrogen atoms (a strong one with the NH<sub>2</sub> group (O...H, 1.74 Å) and a weak one with the amidic proton (O...H, 2.42 Å), in red Fig. 3). The difference between this H-bond pattern and the one displayed in Fig. 1 originates in the lack of templating cations (K<sup>+</sup>, Na<sup>+</sup>), whose presence provokes a small rotation of the guanines in order to firmly interact with the carbonyl groups. Thus, these *in silico* investigations support the PorphySQ design since its structure enables the expected intramolecular G-quartet formation.

### Chemical synthesis

The chemical synthesis of the thus designed PorphySQ was subsequently realized through the pathway described in Fig. 4 (see ESI†). Briefly, the procedure starts with the commercially available 7-bromoheptanenitrile that is converted into 7-bromoheptanal **1** with DIBAL-H (84% chemical yield). Its quadruple condensation on pyrrole, performed in presence of catalytic amounts of BF<sub>3</sub>·Et<sub>2</sub>O provides, after oxidation by DDQ, the tetra-(6-bromohexyl)porphyrin **2**, in a chemical yield that is decent for a porphyrin synthesis (15.5%). This compound is subsequently converted into tetra(6-azidoheptyl)porphyrin **3**, upon treatment with NaN<sub>3</sub> (94% chemical yield), and the terminal azido groups are reduced by LiAlH<sub>4</sub> to provide the tetra-(6-aminoheptyl)porphyrin **4**. This latter porphyrin was found quite tricky to handle, it was consequently decided to make it react, without further purification, with 2-(2-amino-(6-benzoyloxy)-9H-purin-9-yl)acetic acid,<sup>18</sup> under classical peptidic coupling conditions (EDCI, HOBT); the tetra-(10-(6-(2-(2-amino-6-benzoyloxy-9H-purin-9-yl)acetamido)hexyl))porphyrin **5** hereafter named

Prot.PorphySQ is obtained in 42% chemical yield (over 2 steps). The final deprotection, in mild acidic conditions, leads to PorphySQ **6** in high chemical yield (64%) and purity (see ESI†).

### Biophysical evaluations

The quadruplex-recognition properties of PorphySQ were subsequently evaluated: to this end, we employed the FRET-melting assay since it provides reliable and rapid information concerning the ability of a candidate to stabilize a fluorescently labelled quadruplex-forming sequence.<sup>25</sup> This stabilization is estimated *via* the temperature-induced modification of the FRET (fluorescence resonance energy transfer) phenomenon that takes place between two FRET partners (herein FAM (F) and TAMRA (T)), present at both extremities of the studied oligonucleotides. The stabilizing property (*i.e.* the apparent affinity) of a candidate is expressed as an increase in melting temperature ( $\Delta T_{1/2}$ , in °C) imparted by the presence of the ligand. Herein, two different doubly-labelled sequences were used, namely F21T (a 21-nt sequence that mimics the human telomere, FAM-G<sub>3</sub>[T<sub>2</sub>AG<sub>3</sub>]<sub>3</sub>-TAMRA)<sup>7</sup> and F-myc-T (a 22-nt sequence found in the promoter region of c-myc oncogene, FAM-GAG<sub>3</sub>TG<sub>4</sub>AG<sub>3</sub>TG<sub>4</sub>A<sub>2</sub>G-TAMRA).<sup>8</sup> As depicted in Fig. 5A and 5B, in each instance PorphySQ (brown line) displays significantly better stabilizing properties than DOTASQ (red line), with  $\Delta T_{1/2}$  = 6.5 vs. 1.7 °C with F21T, and 8.6 vs. 3.0 °C with F-myc-T. The better results of PorphySQ may originate in its more stable G-quartet fold, due to the self-stabilizing porphyrin ring. To further demonstrate this, and also to be fully confident that the good stabilizing capabilities of PorphySQ do not solely originate in the presence of a porphyrin ring that might interact autonomously with quadruplex, we carried out FRET-melting experiments with F21T in the presence of two other compounds: the ‘naked’ porphyrin **2** (by virtue of its stability, solubility and neutrality) and a porphyrin structurally close to PorphySQ but unable to adopt a closed conformation, *i.e.* Prot.PorphySQ (**5**), in which all guanines are

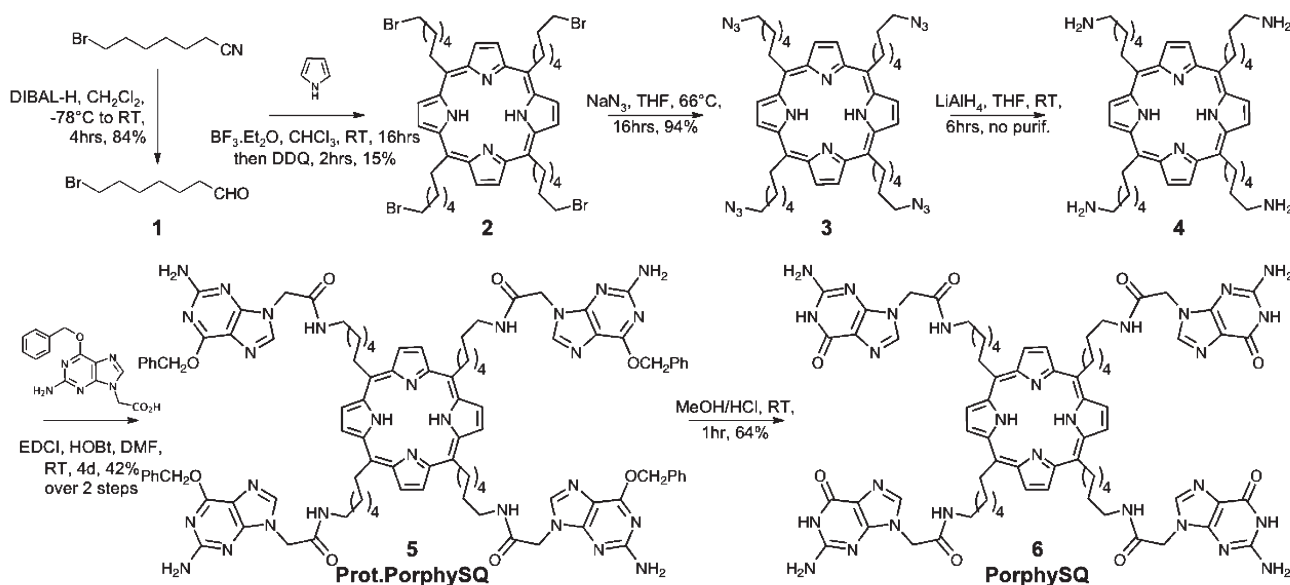
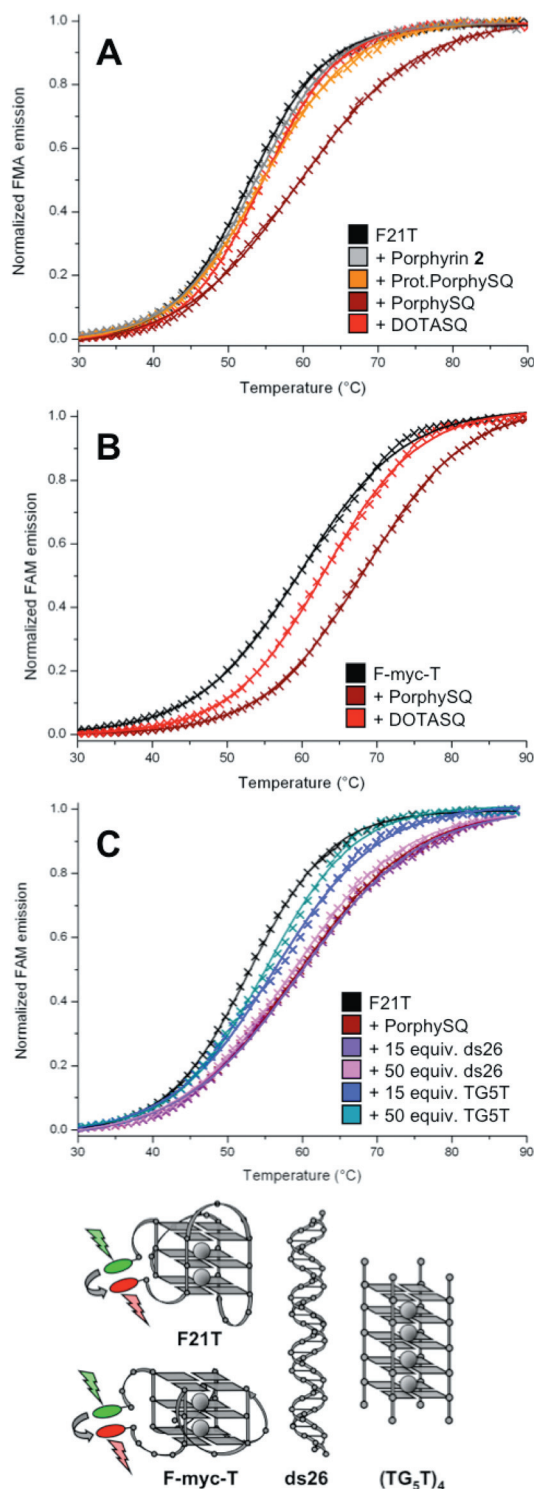


Fig. 4 Chemical synthesis of PorphySQ.





**Fig. 5** FRET-melting experiments with 0.2  $\mu\text{M}$  of F21T (A, C) or F-myc-T (B) in 10 mM lithium cacodylate buffer pH 7.2 plus 10 mM KCl–90 mM LiCl (A, C) or 1 mM KCl–99 mM LiCl (B), without (black curve) or with 5  $\mu\text{M}$  ligand, in absence (PorphyrSQ (brown line), DOTASQ (red line) porphyrin **2** (grey line) and Prot.PorphyrSQ (orange line)) or presence of competitors (ds26, 3 or 10  $\mu\text{M}$  (purple and magenta lines) or  $[\text{TG}_5\text{T}]_4$ , 3 or 10  $\mu\text{M}$  (blue and light blue lines). Lower panel: schematic representation of the oligonucleotides used in this study.

O-protected and thus incapable of forming a G-quartet. As depicted in Fig. 5A, the two compounds (grey lines for **2**, orange line for **5**) impart only a very weak stabilization ( $\Delta T_{1/2} = 0.8$  and  $1.7$   $^{\circ}\text{C}$  respectively), thereby dispelling doubts about the origins of the performances of PorphyrSQ. To gain further insight into its quadruplex-recognition, two competitive FRET-melting experiments were performed: *i*- the first one with ds26, an unlabelled self-complementary 26-nt duplex-DNA ( $\text{CA}_2\text{TCG}_2\text{ATCGA}_2\text{T}_2\text{CGATC}_2\text{GAT}_2\text{G}$ ):<sup>25</sup> as depicted in Fig. 5C (purple and magenta lines), the F21T stabilization imparted by PorphyrSQ is limitedly altered by this high-level competition ( $\Delta T_{1/2} = 6.5$ ,  $6.6$  and  $5.8$   $^{\circ}\text{C}$  with 0, 15 and 50 equiv. of ds26 respectively), implying an elevated selectivity factor ( $S > 0.90$ ); these results confirm the interest in TASQ as G-quadruplex ligands since their shape makes them unable to interact with duplex-DNA;<sup>18</sup> *ii*- the second one with  $[\text{TG}_5\text{T}]_4$ , an unlabelled tetramolecular G-quadruplex with two highly accessible G-quartets: as depicted in Fig. 5C (blue and light blue lines), the PorphyrSQ F21T stabilization is greatly altered by this competition ( $\Delta T_{1/2} = 6.5$ ,  $3.5$  and  $2.3$   $^{\circ}\text{C}$  with 0, 15 and 50 equiv. of  $[\text{TG}_5\text{T}]_4$  respectively), indicating that PorphyrSQ is sensitive to the presence of additional G-quartets and thus that its quadruplex-recognition is certainly mainly driven by G-quartet interaction.<sup>18</sup>

## Conclusions

We herein report on the design and the synthesis of a novel example of water-soluble template-assembled synthetic G-quartet (TASQ) that aims at being implemented as an innovative G-quadruplex ligand. Indeed, we have recently reported on the very first example of a TASQ-based G-quadruplex ligand named DOTASQ (for DOTA-templated synthetic G-quartet), whose interaction with G-quadruplex-DNA was fully original since it hinges on the nature-inspired self-recognition of two G-quartets, one being native (quadruplex) and the other synthetic (TASQ) –a binding mode that we termed ‘like likes like’ approach. Herein, a second example of a G-quartet-based G-quadruplex ligand is reported; in this novel generation, the non-planar DOTA template of DOTASQ is substituted for a porphyrin template: the resulting compound, named PorphyrSQ (for porphyrin-templated synthetic G-quartet) is interesting in that its intramolecular G-quartet fold is not only promoted but also – and above all – stabilized by the  $C_4$ -symmetrical porphyrin template, the porphyrin skeleton being known to be among the most efficient G-quartet binding motifs. The preliminary assessment of the G-quadruplex recognition properties of PorphyrSQ, *via* an array of FRET-melting experiments, demonstrates that this compound displays interesting and promising capabilities, which are also admittedly modest as compared to the best ligands reported so far (including the above-mentioned telomestatin,<sup>11</sup> BRACO-19,<sup>12</sup> Phen-DC<sup>14</sup> and Pyridostatin,<sup>15</sup> which all display very high stabilizing properties (*i.e.*  $\Delta T_{1/2} > 20$   $^{\circ}\text{C}$  at 1  $\mu\text{M}$  dose) in similar experimental conditions).<sup>10,16</sup> These results remain however very interesting since they keep on supporting the hypothesis according to which artificial G-quartets are valuable scaffolds for devising promising G-quadruplex ligands. From now on, we will invest all our efforts into devising novel PorphyrSQ derivatives with enhanced affinity, while keeping the exquisite selectivity of the parent compounds.

## Experimental

### Molecular modelling

**RM1 calculations.** The optimization was carried out without constraint using the semi-empirical RM1 Hamiltonian<sup>23</sup> implemented within the MOPAC2009 program (MOPAC2009, James J. P. Stewart, Stewart Computational Chemistry, Colorado Springs, Co, USA) with the aid of the GABEDIT graphical user interface.<sup>26</sup> The starting geometry was constructed using the HYPERCHEM program (HyperChem8.0.3, Hypercube, Inc., 1115 NW 4th Street, Gainesville, Florida 32601, USA). The minimum energy point was checked by a frequency calculation.

### Synthetic chemistry

**Instrumentation.** <sup>1</sup>H and <sup>13</sup>C NMR spectra were recorded with a Bruker DRX-300 AVANCE transform spectrometer at the "Pôle Chimie Moléculaire (Welience, UB-Filiale)". UV/Vis spectra were recorded with a Varian Cary 1 spectrophotometer. Mass spectra were obtained with a Bruker Daltonics Ultraflex II spectrometer in the MALDI-TOF reflectron mode using dithranol as a matrix or by ESI<sup>+</sup> on a LTQ Orbitrap XL Thermo spectrometer. Accurate mass measurements (HRMS) were carried out under the same conditions as before. The measurements were made at the "Pôle Chimie Moléculaire (Welience, UB-Filiale)".

**Chemicals and reagents.** Unless otherwise noted, all chemicals and solvents were of analytical reagent grade and used as received. Absolute dichloromethane, chloroform and methanol were obtained from Carlo Erba. Silica gel (Merck; 70–120 µm) was used for column chromatography. Analytical thin-layer chromatography was performed with Merck 60 F254 silica gel (precoated sheets, 0.2 mm thick). Reactions were monitored by thin-layer chromatography, UV/Vis spectroscopy and MALDI/TOF mass spectrometry.

**7-Bromoheptanal (1).** 7-Bromoheptanenitrile (2.0 g, 10.52 mmol) was dissolved in 15 mL of dry CH<sub>2</sub>Cl<sub>2</sub> under argon. The solution was cooled to –78 °C and 40 mL of diisobutylaluminium hydride (1.0 M in CH<sub>2</sub>Cl<sub>2</sub>) was added dropwise. The mixture was stirred for 1 h at –78 °C, then warmed to room temperature for 3 h. The reaction was quenched with methanol (20 mL) and 10 mL HCl (10%) was added dropwise at –78 °C. The product was extracted with ether (3 × 100 mL) and washed with distilled water then brine. The solvent was removed by evaporation under reduced pressure to lead to compound **1** in 84% yield (1.7 g, 8.80 mmol). <sup>1</sup>H NMR (CDCl<sub>3</sub>) δ (ppm): 9.79 (s, 1H), 3.42 (t, 2H, <sup>3</sup>J<sub>HH</sub> = 6.0 Hz), 2.46 (m, 2H), 1.88 (m, 2H), 1.67 (m, 2H), 1.40 (m, 4H).

**Tetra(6-bromohexyl)porphyrin (2).** Under nitrogen, 3 mmol of 7-bromoheptanal **1** (0.58 g) and 3 mmol of pyrrole (0.20 g) were dissolved in 200 mL of chloroform. The solution was purged by nitrogen for 2 h. Still under nitrogen, 75 µL of BF<sub>3</sub>·Et<sub>2</sub>O were added to the solution at 20 °C. The mixture was stirred overnight. DDQ (3 mmol) was added and the mixture was again stirred for 2 h, then two drops of triethylamine were added. The solvent was removed under reduced pressure. The product was purified by column chromatography on silica gel

using CH<sub>2</sub>Cl<sub>2</sub> as eluent and recrystallized from CHCl<sub>3</sub>–CH<sub>3</sub>OH. Yield: 15.5% (112 mg, 0.465 mmol). <sup>1</sup>H NMR (CDCl<sub>3</sub>) δ (ppm): 9.48 (s, 8H, H-pyrro), 4.97 (t, 8H, <sup>3</sup>J<sub>HH</sub> = 6.0 Hz, α-CH<sub>2</sub>–), 3.45 (t, 8H, <sup>3</sup>J<sub>HH</sub> = 6.0 Hz, Br–CH<sub>2</sub>–), 2.55 (m, 8H, β-CH<sub>2</sub>–), 1.97 (m, 8H, γ-CH<sub>2</sub>–), 1.82 (m, 8H, δ-CH<sub>2</sub>–), 1.68 (m, 8H, ε-CH<sub>2</sub>–), –2.64 (s, 2H, N–H). <sup>13</sup>C NMR (CDCl<sub>3</sub>) δ (ppm): 144.8, 128.6 (broad s), 118.1, 38.2, 35.3, 34.0, 32.9, 29.6, 28.2. MS (MALDI-TOF) *m/z* = 957.96 [M]<sup>+</sup>, 958.14 calcd for C<sub>44</sub>H<sub>58</sub>Br<sub>4</sub>N<sub>5</sub>. UV-Vis (CH<sub>2</sub>Cl<sub>2</sub>): λ<sub>max</sub> (nm) (ε × 10<sup>–3</sup> L mol<sup>–1</sup> cm<sup>–1</sup>) = 416.9 (440.7), 519.0 (14.9), 554.0 (9.8), 600.1 (4.3), 658.1 (7.3).

**Tetra(6-azidoheptyl)porphyrin (3).** In 20 mL of THF were dissolved 100 mg (0.104 mmol) of tetra(6-bromohexyl)porphyrin **2**, then 2 mL of H<sub>2</sub>O containing 56 mg of NaN<sub>3</sub> were added to the solution. The mixture was heated to 66 °C overnight. The solvent was removed under reduced pressure. The residue was dissolved in 100 mL CHCl<sub>3</sub>. The organic solution was washed with H<sub>2</sub>O (3 × 10 mL) and dried over MgSO<sub>4</sub>. The organic solvent was then removed under reduced pressure. The product was purified by column chromatography on silica gel with CH<sub>2</sub>Cl<sub>2</sub>–heptane (8:2) as eluent then recrystallized from CHCl<sub>3</sub>–CH<sub>3</sub>OH. Yield: 94% (80 mg, 0.098 mmol). <sup>1</sup>H NMR (CDCl<sub>3</sub>) δ (ppm): 9.49 (s, 8H, H-pyrro), 4.93 (t, 8H, <sup>3</sup>J<sub>HH</sub> = 9.0 Hz, α-CH<sub>2</sub>–), 3.30 (t, 8H, <sup>3</sup>J<sub>HH</sub> = 6.0 Hz, N<sub>3</sub>–CH<sub>2</sub>–), 2.53 (m, 8H, –CH<sub>2</sub>–), 1.81 (m, 8H, –CH<sub>2</sub>–), 1.65 (m, 16H, –CH<sub>2</sub>–), –2.65 (s, 2H, N–H). <sup>13</sup>C NMR (CDCl<sub>3</sub>) δ (ppm): 144.7, 128.3 (broad s), 118.1, 51.5, 38.3, 35.3, 29.9, 28.9, 26.8. MS (MALDI-TOF) *m/z* = 810.50 [M]<sup>+</sup>, 810.50 calcd for C<sub>44</sub>H<sub>58</sub>N<sub>16</sub>. UV-Vis (CH<sub>2</sub>Cl<sub>2</sub>): λ<sub>max</sub> (nm) (ε × 10<sup>–3</sup> L mol<sup>–1</sup> cm<sup>–1</sup>) = 416.0 (408.6), 519.0 (14.9), 554.0 (9.8), 601.0 (4.0), 658.9 (7.2).

**Tetra(6-aminoheptyl)porphyrin (4).** Under argon, 70 mg (0.086 mmol) of tetra(6-azidoheptyl)porphyrin **3** was dissolved in 5 mL of dry THF and cooled to 0 °C. LiAlH<sub>4</sub> (30 mg, 0.79 mmol) in 3 mL of dry THF was added slowly to the solution. The reaction mixture was heated to room temperature and stirred for 6 h and 0.5 mL of ethanol was added to quench the reaction. Then 50 mL of water was added. The porphyrin was extracted with CHCl<sub>3</sub> (3 × 50 mL). The collected organic solution was washed with H<sub>2</sub>O, brine and dried over MgSO<sub>4</sub>. The solution was concentrated to about 3 mL and used directly in the next step without any further purification. <sup>1</sup>H NMR (CDCl<sub>3</sub>) δ (ppm): 9.39 (s, 8H, H-pyrro), 4.87 (t, 8H, <sup>3</sup>J<sub>HH</sub> = 8.1 Hz, α-CH<sub>2</sub>–), 2.64 (t, 8H, <sup>3</sup>J<sub>HH</sub> = 6.6 Hz, NH<sub>2</sub>–CH<sub>2</sub>–), 2.45 (m, 8H, –CH<sub>2</sub>–), 1.74 (m, 8H, –CH<sub>2</sub>–), 1.46 (m, 16H, –CH<sub>2</sub>–), –2.70 (s, 2H, N–H). MS (MALDI-TOF) *m/z* = 706.36 [M]<sup>+</sup>, 706.54 calcd for C<sub>44</sub>H<sub>66</sub>N<sub>8</sub>.

**Prot.PorphSQ (5).** DMF (7 mL) was added to the above solution of tetra(6-aminoheptyl)porphyrin **4**. Then 2-(2-amino-6-(benzyloxy)-9H-purin-9-yl)acetic acid (110 mg, 0.367 mmol), *N*-hydroxybenzotriazole (HOBt) (56 mg, 0.367 mmol) and 1-ethyl-3-(3-dimethylaminopropyl)carbodiimide (EDCI) (70.5 mg, 0.367 mmol) were added. The resulting mixture was stirred at 20 °C for 4 d. After the solvent was removed under reduced pressure, the residue was washed with water, a saturated aqueous solution of NaHCO<sub>3</sub>, CH<sub>2</sub>Cl<sub>2</sub>, ethyl acetate and methanol repeatedly to give compound **5** as a solid. Yield: 42% (65 mg,

0.036 mmol).  $^1\text{H}$  NMR ( $\text{CDCl}_3$ )  $\delta$  (ppm): 9.67 (s, 8H), 8.14 (t, 4H,  $^3J_{\text{HH}} = 6.0$  Hz), 7.77 (s, 4H), 7.46–7.31 (m, 20H), 6.38 (s, 8H), 5.45 (s, 8H), 4.96 (m, 8H), 4.67 (s, 8H), 3.12 (d, 8H,  $J_{\text{HH}} = 3.0$  Hz), 2.41 (m, 8H), 1.77 (m, 8H), 1.50 (m, 16H), –2.89 (s, 2H). MS (MALDI-TOF)  $m/z = 1832.04$   $[\text{M}]^+$ , 1832.12 calcd for  $\text{C}_{100}\text{H}_{110}\text{N}_{28}\text{O}_8$ . HR-MS (ESI)  $m/z = 1853.8960$   $[\text{M} + \text{Na}]^+$ , 1853.8953 calcd for  $\text{C}_{100}\text{H}_{110}\text{N}_{28}\text{NaO}_8$ . UV-Vis (DMF):  $\lambda_{\text{max}}$  (nm) ( $\epsilon \times 10^{-3} \text{ L mol}^{-1} \text{ cm}^{-1}$ ) = 416.0 (242.0), 519.0 (9.9), 552.0 (6.9), 600.9 (2.9), 658.9 (5.6).

**PorphySQ (6).** Protected porphyrin **5** (35.0 mg, 0.019 mmol) was taken up in a solution of MeOH saturated by HCl (20 mL). The mixture was stirred at 20 °C for 1 h. The final product was precipitated by addition of diethyl ether (80 mL), and washed repeatedly with ether (20 mL). Porphyrin **6** was obtained as a solid. Yield: 63% (18 mg, 0.012 mmol).  $^1\text{H}$  NMR (DMSO)  $\delta$  (ppm): 11.01 (s, 4H), 9.67 (s, 8H), 8.29 (s, 8H), 6.75 (s, 8H), 4.97 (s, 16H), 4.73 (s, 8H), 3.05 (s, 8H), 1.80 (s, 8H), 1.49 (s, 16H), –2.89 (s, 2H).  $^{13}\text{C}$  NMR (DMSO)  $\delta$  (ppm): 164.7, 152.2, 153.8, 150.1, 138.2, 128.9 (broad s), 108.5, 45.7, 34.6, 29.4, 28.9, 26.4. HR-MS (ESI)  $m/z = 1493.7011$   $[\text{M} + \text{Na}]^+$ , 1493.7076 calcd for  $\text{C}_{72}\text{H}_{86}\text{N}_{28}\text{NaO}_8$ . UV-Vis (DMSO):  $\lambda_{\text{max}}$  (nm) ( $\epsilon \times 10^{-3} \text{ L mol}^{-1} \text{ cm}^{-1}$ ) = 418.0 (238.0), 519.0 (10.0), 554.0 (6.4), 600.0 (2.5), 659.0 (4.0).

### FRET-melting assay

**Oligonucleotides.** Labelled (F21T and F-myc-T) and unlabelled oligonucleotides (ds26 and TG5T) were purchased from Eurogentec (Belgium) in OligoGold purity grade at ~200 nmol scale (purified by RP-HPLC). Oligonucleotides were prepared by mixing 40  $\mu\text{L}$  of mother solution (500  $\mu\text{M}$  in strands (except for TG5T at 2 mM in strands) in deionized water (18.2 M $\Omega$  cm resistivity)), 152  $\mu\text{L}$  of a 100 mM KCl–900 mM LiCl solution, 152  $\mu\text{L}$  of a lithium cacodylate solution (100 mM, pH 7.2) and 456  $\mu\text{L}$  of water. The final concentration of the prepared aliquots was theoretically 25  $\mu\text{M}$  for quadruplex-DNA and 50  $\mu\text{M}$  for ds26 in a Caco.K buffer solution (comprised of 10 mM lithium cacodylate buffer (pH 7.2) + 10 mM KCl–90 mM LiCl) and diluted aliquots (~2.5  $\mu\text{M}$ ) were obtained by addition of Caco.K buffer. The actual concentrations of aliquots were evaluated *via* UV-Vis spectra analysis at 260 nm and 90 °C, using the molar extinction coefficient value provided by the manufacturer. The higher-order structures of the aliquots were obtained by heating the solutions at 90 °C for 5 min, cooling in ice for 6 h to favour the intramolecular folding, and then were stored at least overnight at 4 °C (except for both  $[\text{TG}_5\text{T}]_4$  and ds26, obtained by heating the solution at 90 °C for 5 min, cooling at 65 °C for 120 min, 50 °C for 90 min, 35 °C for 60 min, 20 °C for 60 min and finally stored at 4 °C). Prior to use, typical diluted solutions were F21T: 2.75  $\mu\text{M}$ , F-myc-T: 3.39  $\mu\text{M}$ , ds26: 51  $\mu\text{M}$  and  $[\text{TG}_5\text{T}]_4$ : 245  $\mu\text{M}$ .

**FRET-melting protocol.** Experiments were performed as a high-throughput screen in a 96-well format, with F21T (FAM- $5'$ G $_3$ T $_2$ AG $_3$ T $_2$ AG $_3$ T $_2$ AG $_3$ -TAMRA, with FAM (F): 6-carboxy-fluorescein and TAMRA (T): 6-carboxy-tetramethylrhodamine) and F-myc-T (FAM- $5'$ GAG $_3$ TG $_4$ AG $_3$ TG $_4$ A $_2$ G $_3$ -TAMRA). Fluorescence melting curves were determined with an Agilent

Stratagene Mx3005P real-time PCR machine, using a total reaction volume of 100  $\mu\text{L}$ , with 0.2  $\mu\text{M}$  of tagged oligonucleotide in a buffer containing 10 mM lithium cacodylate pH 7.2 plus 10 mM KCl–90 mM LiCl (for F21T) or 1 mM KCl–99 mM LiCl (for F-myc-T). After a first equilibration step at 25 °C during 30 s, a stepwise increase of 1 °C every 30 s for 65 cycles to reach 90 °C was performed and measurements were made after each cycle with excitation at 492 nm and detection at 516 nm. The melting of the G-quadruplex was monitored alone or in the presence of various concentrations of compounds and/or of competitor, either the self-complementary duplex-forming sequence ds26 ( $5'$ CA $_2$ TCG $_2$ ATCGA $_2$ T $_2$ CGATC $_2$ GAT $_2$ G $_3$ ) or the tetramolecular-quadruplex-forming TG $_5$ T sequence (*vide infra*). Final analysis of the data was carried out using Excel and OriginPro.8. Emission of FAM was normalized between 0 and 1, and  $T_{1/2}$  was defined as the temperature for which the normalized emission is 0.5.  $\Delta T_{1/2}$  values are mean of 2 to 4 experiments.

**Competitive FRET-melting experiments.** Experiments were carried out with 15 and 50 equiv. of both ds26 and  $[\text{TG}_5\text{T}]_4$ , expressed in motif concentrations: ds26 being a self-complementary duplex-DNA, the experiments were thus carried out with 30 and 100 equiv. expressed in strand concentration, which corresponds to 6 and 20  $\mu\text{M}$  actual ds26 strand concentration;  $[\text{TG}_5\text{T}]_4$  being a tetramolecular-quadruplex-forming sequence, the experiments were thus carried out with 60 and 200 equiv. expressed in strand concentration, which corresponds to 12 and 40  $\mu\text{M}$  actual TG $_5$ T strand concentration. Of note, ds26 and  $[\text{TG}_5\text{T}]_4$  have been selected since their melting temperature ( $T_m$ , evaluated by UV-melting experiments) are >20 °C above that of F21T ( $T_m = 79$  and >80 °C for ds26 and  $[\text{TG}_5\text{T}]_4$  respectively in 10 mM lithium cacodylate pH 7.2 plus 10 mM KCl/90 mM LiCl).

### Acknowledgements

The authors thank F. Cuenot for help with funding, CheMatech® company for the assistance in DOTASQ synthesis, the CNRS, Université de Bourgogne and Conseil Régional de Bourgogne (3MIM project (FD, CPG, DM)) and the Agence Nationale de la Recherche (ANR-10-JCJC-0709 (DM)).

### Notes and references

- 1 J. T. Davis, *Angew. Chem., Int. Ed.*, 2004, **43**, 668.
- 2 M. Duca, P. Vekhoff, K. Oussedik, L. Halby and P. B. Arimondo, *Nucleic Acids Res.*, 2008, **36**, 5123.
- 3 J. T. Davis and G. P. Spada, *Chem. Soc. Rev.*, 2007, **36**, 296.
- 4 C. W. Collie and G. N. Parkinson, *Chem. Soc. Rev.*, 2011, **40**, 5867.
- 5 S. Burge, G. N. Parkinson, P. Hazel, A. K. Todd and S. Neidle, *Nucleic Acids Res.*, 2006, **34**, 5402; D. J. Patel, A. T. Phan and V. Kuryavii, *Nucleic Acids Res.*, 2007, **35**, 7429; D. Yang and K. Okamoto, *Future Med. Chem.*, 2010, **2**, 619.
- 6 A. K. Todd, M. Johnston and S. Neidle, *Nucleic Acids Res.*, 2005, **33**, 2901; J. L. Huppert and S. Balasubramanian, *Nucleic Acids Res.*, 2005, **33**, 2908.
- 7 Y. Xu, *Chem. Soc. Rev.*, 2011, **40**, 2719; S. Neidle, *FEBS J.*, 2010, **277**, 1118; A. De Cian, L. Lacroix, C. Douarre, N. Temime-Smaali, C. Trentesaux, J.-F. Riou and J.-L. Mergny, *Biochimie*, 2008, **90**, 131.
- 8 S. Balasubramanian, L. H. Hurley and S. Neidle, *Nat. Rev. Drug Discovery*, 2011, **10**, 261.
- 9 A. Bugaut and S. Balasubramanian, *Nucleic Acids Res.*, 2012, **40**, 4727.



- 10 S. Balasubramanian and S. Neidle, *Curr. Opin. Chem. Biol.*, 2009, **13**, 345.
- 11 K. Shin-ya, K. Wierzbza, K.-I. Matsuo, T. Ohtani, Y. Yamada, K. Furihata, Y. Hayakawa and H. Seto, *J. Am. Chem. Soc.*, 2001, **123**, 1262; N. Temime-Smaali, L. Guittat, A. Sidibe, K. Shin-ya, C. Trentesaux and J.-F. Riou, *PLoS One*, 2009, **4**, e6919.
- 12 M. J. B. Moore, C. M. Schultes, J. Cuesta, F. Cuenca, M. Gunaratnam, F. A. Tanious, W. D. Wilson and S. Neidle, *J. Med. Chem.*, 2006, **49**, 582; M. Gunaratnam, O. Greciano, C. Martins, A. P. Reszka, C. M. Schultes, H. Morjani, J.-F. Riou and S. Neidle, *Biochem. Pharmacol.*, 2007, **74**, 679.
- 13 P. Phatak, J. C. Cookson, F. Dai, V. Smith, R. B. Gartenhaus, M. F. G. Stevens and A. M. Burger, *Br. J. Cancer*, 2007, **96**, 1223; E. Salvati, M. Scarsella, M. Porru, A. Rizzo, S. Iachettini, L. Tentori, G. Graziani, M. D'Incalci, M. F. G. Stevens, A. Orlandi, D. Passeri, E. Gilson, G. Zupi, C. Leonetti and A. Biroccio, *Oncogene*, 2010, **29**, 6280.
- 14 A. De Cian, E. DeLemos, J.-L. Mergny, M.-P. Teulade-Fichou and D. Monchaud, *J. Am. Chem. Soc.*, 2007, **129**, 1856; A. De Cian, G. Cristofari, P. Reichenbach, E. DeLemos, D. Monchaud, M.-P. Teulade-Fichou, K. Shin-ya, L. Lacroix, J. Lingner and J.-L. Mergny, *Proc. Natl. Acad. Sci. U. S. A.*, 2007, **104**, 17347.
- 15 R. Rodriguez, S. Müller, J. A. Yeoman, C. Trentesaux, J.-F. Riou and S. Balasubramanian, *J. Am. Chem. Soc.*, 2008, **130**, 15758; R. Rodriguez, K. M. Miller, J. V. Forment, C. R. Bradshaw, M. Nikan, S. Britton, T. Oelschlaegel, B. Xhemalce, S. Balasubramanian and S. P. Jackson, *Nat. Chem. Biol.*, 2012, **8**, 301.
- 16 D. Monchaud and M.-P. Teulade-Fichou, *Org. Biomol. Chem.*, 2008, **6**, 627; S. Neidle, *Curr. Opin. Struct. Biol.*, 2009, **19**, 239.
- 17 A. Bugaut, R. Rodriguez, S. Kumari, S.-T. D. Hsu and S. Balasubramanian, *Org. Biomol. Chem.*, 2010, **8**, 2771; D. Gomez, A. Guédin, J.-L. Mergny, B. Salles, J.-F. Riou, M.-P. Teulade-Fichou and P. Calsou, *Nucleic Acids Res.*, 2010, **38**, 7187; K. Halder, E. Lary, M. Benzler, M.-P. Teulade-Fichou and J. S. Hartig, *ChemBioChem*, 2011, **12**, 1663.
- 18 L. Stefan, A. Guédin, S. Amrane, N. Smith, F. Denat, J.-L. Mergny and D. Monchaud, *Chem. Commun.*, 2011, **47**, 4992; L. Stefan, H.-J. Xu, C. P. Gros, F. Denat and D. Monchaud, *Chem.-Eur. J.*, 2011, **17**, 10857; L. Stefan, F. Denat and D. Monchaud, *J. Am. Chem. Soc.*, 2011, **133**, 20405.
- 19 M. Nikan and J. C. Sherman, *Angew. Chem., Int. Ed.*, 2008, **47**, 4900.
- 20 M. Nikan and J. C. Sherman, *J. Org. Chem.*, 2009, **74**, 5211; M. Nikan, G. A. L. Bare and J. C. Sherman, *Tetrahedron Lett.*, 2011, **52**, 1791.
- 21 P. Murat, R. Bonnet, A. Van der Heyden, N. Spinelli, P. Labbé, D. Monchaud, M.-P. Teulade-Fichou, P. Dumy and E. Defrancq, *Chem.-Eur. J.*, 2010, **16**, 6106; P. Murat, B. Gennaro, J. Garcia, N. Spinelli, P. Dumy and E. Defrancq, *Chem.-Eur. J.*, 2011, **17**, 5791.
- 22 D. Monchaud, A. Granzhan, N. Saettel, A. Guédin, J.-L. Mergny and M.-P. Teulade-Fichou, *J. Nucl. Acids*, 2010, **2010**, ID525862.
- 23 G. B. Rocha, R. O. Freire, A. M. Simas and J. J. P. Stewart, *J. Comput. Chem.*, 2006, **10**, 1101.
- 24 J. Gu and J. Leszczynski, *J. Phys. Chem. A*, 2000, **104**, 6308.
- 25 A. De Cian, L. Guittat, M. Kaiser, B. Saccà, S. Amrane, A. Bourdoncle, P. Alberti, M.-P. Teulade-Fichou, L. Lacroix and J.-L. Mergny, *Methods*, 2007, **42**, 183.
- 26 A. R. Allouche, *J. Comput. Chem.*, 2011, **32**, 174.